Flow and Heat Transfer Analysis of Copper-water Nanofluid with Temperature Dependent Viscosity Past a Riga Plate

A. Ahmad, S. Ahmed, and F. M. Abbasi*

Department of Mathematics, COMSATS Institute of Information Technology, Islamabad 44000, Pakistan

Flow of electrically conducting nanofluids is of pivotal importance in countless industrial and medical appliances. Fluctuations in thermophysical properties of such fluids due to variations in temperature have not received due attention in the available literature. Present investigation aims to fill this void by analyzing the flow of copper-water nanofluid with temperature dependent viscosity past a Riga plate. Strong wall suction and viscous dissipation have also been taken into account. Numerical solutions for the resulting nonlinear system have been obtained. Results are presented in the graphical and tabular format in order to facilitate the physical analysis. An estimated expression for skin friction coefficient and Nusselt number are obtained by performing linear regression on numerical data for embedded parameters. Results indicate that the temperature dependent viscosity alters the velocity as well as the temperature of the nanofluid and is of considerable importance in the processes where high accuracy is desired. Addition of copper nanoparticles makes the momentum boundary layer thinner whereas viscosity parameter does not affect the boundary layer thickness. Moreover, the regression expressions indicate that magnitude of rate of change in effective skin friction coefficient and Nusselt number with respect to nanoparticles volume fraction is prominent when compared with the rate of change with variable viscosity parameter and modified Hartmann number.

Keywords : temperature dependent viscosity, copper-water nanofluid, riga plate, regression relations

1. Introduction

Nanofluids play central role in modern engineering appliances. Due to their unique chemical and thermophysical properties such fluids are preferred over conventional fluids in industrial processes involving heat transfer. Many such processes make use of high effective thermal conductivity of nanofluids to facilitate heat transfer and to prevent energy loss. Nanofluids are readily being used in domestic and industrial cooling systems, IT industry, geothermal energy extraction, solar panels, cellular and automobile industries, magnetic drug delivery systems and many other industrial and medical processes to enhance their efficiency. Such wide utilization of nanofluids is the chief reason behind the ever growing interest of motivated researchers in the analysis of such fluids. Since the innovative idea of nanofluids proposed by Choi [1], several investigations have been carried out to examine

different aspects of such fluid, some of which can be seen through Refs. [2-12].

Flows governed by wall motion and wall suction find large number of applications in industry. In such flows, thickness of momentum boundary layer can be controlled by the motion and porosity of the wall. On the other hand, electromagnetic forces play central role in controlling boundary layer thickness in hydromagnetic flows. Fluids with high electric thermal conductivities are governed by classical MHD flows. Contrary to this, currents produced by externally applied magnetic fields alone are not sufficient to generate flow in weakly conducting fluid. In order to achieve an effective flow control external electric field must be added. To generate simultaneous electric and magnetic fields Gailitis and Lielausis [13] introduced the Riga plate which can produce Lorentz force parallel to the wall which in turn is helpful in flow control. The term for the wall-parallel Lorentz force named Grinberg-term [14] is negative exponential function of direction normal to the plate. Recently Ahmad *et al.* [15] examined the flow of nanofluid past a Riga plate. In this study authors used the Bongiorno's model [2] for the analysis of nano-

*Corresponding author: Tel: +92-9049-5557
Fax: +92-9049-5558, e-mail: abbasisarkar@gmail.com

fluid.

It is well established fact that the temperature of a fluid perturbs its thermophysical properties. Such variations in thermophysical properties of a fluid with temperature become additionally important when high accuracy is desired. Several analysts have used Brinkmann's model [16] for the viscosity of two phase flows in their analysis of nanofluids. Although this model takes into account the effect of nanoparticles volume fraction on the viscosity, yet the dependence of temperature is ignored at once. Despite of sizeable literature available on the mechanical analysis of nanofluids, not much has been said about flow of nanofluids with temperature dependent viscosity. This study aims to plug this gap by combining the Brinkman's viscosity model with the exponential model of the temperature dependent viscosity.

Flow of electrically conducting nanofluid past a Riga-late with strong suction is investigated here. The nanofluid is composed of water and copper nanoparticles. Viscosity if the nanofluid is taken to be temperature dependent. Viscous dissipation is also taken into account. Resulting nonlinear system is solved numerically. Obtained results are presented graphically for physical analysis. Analytical expressions are developed for skin friction and Nusselt number by performing linear regression on the obtained numerical data. Comparison for the case of constant and variable viscosity is also presented with the anticipation that this study will serve as a reference for future research in the field.

2. Mathematical Formulation

Consider the flow of electrically conducting fluid containing nanoparticles induced by a Riga plate placed at $y = 0$ with x-axis aligned vertically upward. The Riga plate consists of an alternating array of electrodes and
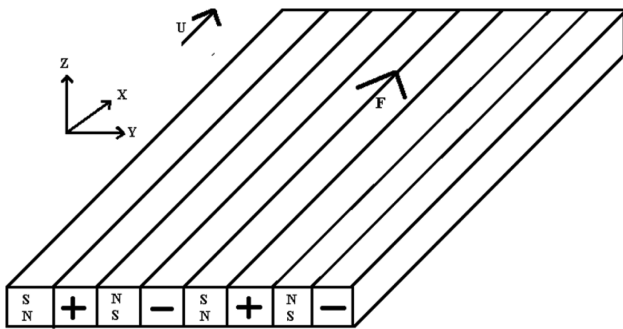
Fig. 1. Sketch of a Riga plate consisting of an alternating array of electrodes and permanent magnets. The Lorentz force and the mainstream velocity are parallel to the array.

permanent magnets mounted on a plane surface (see Figure 1). Employing the Oberbeck-Boussinesq approximation and the assumption that the nanoparticles concentration is dilute, the boundary layer equations for the conservation of total mass, momentum and thermal energy are written as:

$$\frac{\partial U}{\partial X} + \frac{\partial V}{\partial Y} = 0 , \tag{1}$$

$$\rho_{eff}\left(U\frac{\partial U}{\partial X} + V\frac{\partial U}{\partial Y}\right) = \frac{\partial}{\partial Y}\left(\mu_{eff}\frac{\partial U}{\partial Y}\right) + g(\rho\beta)_{eff}(T - T_\infty)$$
$$+ \frac{\pi j_o M_o}{8}\exp\left(-\frac{\pi}{a}y\right), \tag{2}$$

$$(\rho C_{eff})\left(U\frac{\partial T}{\partial X} + V\frac{\partial T}{\partial Y}\right) = K_{eff}\frac{\partial^2 T}{\partial Y^2} , \tag{3}$$

The plate with suction velocity V_o is assumed to move in x direction with constant velocity. At the sheet the temperature T takes the constant value T_w. The ambient value of T is given as T_∞. The boundary conditions may be written as:

$$U = U_w, V = V_w, T = T_w \text{ at } Y = 0$$
$$U(X, Y) \rightarrow 0, \ T = T_\infty \text{ as } Y \rightarrow \infty \tag{4}$$

In Eqs. (1)-(4), (U, V) are the velocity components in (X, Y) directions respectively. $j_o(A/m^2)$ is the applied current density in the electrodes, M_o (Tesla) is the magnetization of the permanent magnets and a is the width of magnets and electrodes. In Eq. (2), the last term known as Grinberg-term represents the wall-parallel Lorentz force and is fully decoupled from the flow and decreases exponentially in the direction normal to the plate. Relations for effective heat capacity $(\rho C)_{eff}$, effective density ρ_{eff}, effective viscosity μ_{eff} [16], effective thermal expansion $(\rho\beta)_{eff}$, and effective thermal conductivity K_{eff} of the nanofluid are given as follows:

$$\frac{K_{eff}}{K_f} = \frac{K_p + 2K_f - 2\phi(K_f - K_p)}{K_p + 2K_f + \phi(K_f - K_p)}, \mu_{eff} = \frac{\mu_f(1 - \alpha_1(T - T_0))}{(1 - \phi)^{2.5}} \tag{5}$$

$$\rho_{eff} = (1 - \phi)\rho_f + \phi\rho_p, (\rho C)_{eff} = (1 - \phi)(\rho C)_f + \phi(\rho C)_p ,$$
$$(\rho C)_{eff} = (1 - \phi)(\rho\beta)_f + \phi(\rho\beta)_p . \tag{6}$$

In these equations ρ, C, β and ϕ are the density, specific heat, thermal expansion coefficient, electric conductivity, and nano particle volume fraction respectively and the subscripts 'p' and 'f' denote the nanoparticles and fluid phase respectively. Introducing the non-dimensional parameters

$$x = \frac{X}{l}, y = \frac{Y}{L}, u = \frac{U}{U_w}, v = \frac{V}{V_o}, \theta = \frac{T - T_\infty}{T_w - T_\infty},$$

$$L = \frac{a}{\pi}, l = \frac{U_w L^2}{\upsilon}, V_o = \frac{\upsilon \pi}{a} \qquad (7)$$

in the Eqs. (1)-(4) and obtain the non-dimensional form as:

$$\frac{\partial u}{\partial x} + \frac{\partial v}{\partial y} = 0 \qquad (8)$$

$$(1 + (\bar{\rho} - 1)\varphi)\left(u\frac{\partial u}{\partial x} + v\frac{\partial u}{\partial y} \right) = \frac{\partial}{\partial y}\left(\frac{1 - \alpha\theta}{(1-\varphi)^{2.5}}\frac{\partial u}{\partial y} \right)$$
$$+ \lambda(1 + (\bar{\rho}\bar{\beta} - 1)\varphi)\theta + Ze^{-y}, \qquad (9)$$

$$(1 + (\bar{\rho}\bar{C} - 1)\varphi)\left(u\frac{\partial \theta}{\partial x} + v\frac{\partial \theta}{\partial y} \right) = \frac{A}{\Pr}\frac{\partial^2 \theta}{\partial y^2} + \frac{1 - \alpha\theta}{(1-\varphi)^{2.5}}\left(\frac{\partial u}{\partial y} \right)^2, \quad (10)$$

with boundary conditions

$$u = 1, \ v = v_w, \ \theta = 1 \text{ at } y = 0$$
$$u(x,y) \to 0, \quad \theta = 0 \text{ as } y \to \infty \qquad (11)$$

In the above equations λ is the Richardson number, Z is the modified Hartmann number, $\Pr$ is the Prandtl's number, υ is the kinematic viscosity of the fluid, given as:

$$\lambda = \frac{a^2 \Delta T}{\pi^2 \upsilon U_w} g\beta, \ \ Z = \frac{1}{8\pi}\frac{a^2 j_o M_o}{U_w \mu_f}, \ \ \Pr = \frac{\upsilon(\rho C)_f}{K_f}$$
$$\upsilon = \frac{\mu_f}{\rho_f}, A = \frac{K_p + 2K_f - 2\phi(K_f - K_p)}{K_p + 2K_f + \phi(K_f - K_p)} \qquad (12)$$

With assumption of strong suction/injection [17] Eqs. (9)-(11) can be rewritten as:

$$\frac{\partial v}{\partial y} = 0, \qquad (13)$$

$$(1 + (\bar{\rho} - 1)\varphi)v\frac{\partial u}{\partial x} = \frac{\partial}{\partial y}\left(\frac{1 - \alpha\theta}{(1-\varphi)^{2.5}}\frac{\partial u}{\partial y} \right)$$
$$+ \lambda(1 + (\bar{\rho}\bar{\beta} - 1)\varphi)\theta + Ze^{-y}, \qquad (14)$$

$$\left(1 + (\bar{\rho}\bar{C} - 1)\varphi \right)v\frac{\partial \theta}{\partial y} = \frac{A}{\Pr}\frac{\partial^2 \theta}{\partial y^2} + \frac{1 - \alpha\theta}{(1-\varphi)^{2.5}}\left(\frac{\partial u}{\partial y} \right)^2, \quad (15)$$

Continuity equation and condition $v = v_w$ at $y = 0$ implies $v = v_w$. Thus the governing equations may be written as:

$$(1 + (\bar{\rho} - 1)\varphi)v_w\frac{\partial u}{\partial y} = \frac{\partial}{\partial y}\left(\frac{1 - \alpha\theta}{(1-\varphi)^{2.5}}\frac{\partial u}{\partial y} \right)$$
$$+ \lambda(1 + (\bar{\rho}\bar{\beta} - 1)\varphi)\theta + Ze^{-y}, \qquad (16)$$

$$\left(1 + (\bar{\rho}\bar{C} - 1)\varphi \right)v_w\frac{\partial \theta}{\partial y} = \frac{A}{\Pr}\frac{\partial^2 \theta}{\partial y^2} + \frac{1 - \alpha\theta}{(1-\varphi)^{2.5}}\left(\frac{\partial u}{\partial y} \right)^2, \quad (17)$$

where for the suction velocity we write $v_w = -s$, $s > 0$. Corresponding boundary conditions are

$$u = 1, \ \theta = 1 \text{ at } y = 0$$
$$u(x,y) \to 0, \quad \theta = 0 \text{ as } y \to \infty \qquad (18)$$

3. Solution Methodology

To solve the boundary value problem (16)-(18) numerically, nonlinear shooting method is adopted. Shooting technique is used to guess the initial condition of converted initial value problem such that it satisfies the boundary conditions of original boundary value problem. The resulting differential equations can then be integrated using initial value solver like Runge-Kutta technique.

The skin friction coefficient, a physical quantity of practical interest, is defined as:

$$C_f = \frac{\tau_w}{\rho_{eff}U_w^2}, \qquad (19)$$

where τ_w is the shear stress at the surface

$$\tau_w = \mu_{eff}\frac{\partial U}{\partial Y}\bigg|_{Y=0}. \qquad (20)$$

In dimensionless form, it yields:

$$\tau_w = \frac{\mu_{of}U_w}{L}\frac{1 - \alpha\theta}{(1-\varphi)^{2.5}}\frac{\partial u}{\partial y}\bigg|_{y=0}, \qquad (21)$$

$$C_f \operatorname{Re} = \frac{1}{1 + (\bar{\rho} - 1)\varphi}\frac{1 - \alpha\theta}{(1-\varphi)^{2.5}}\frac{\partial u}{\partial y}\bigg|_{y=0}. \qquad (22)$$

Similarly, Nusselt number (Nu) is defined as

$$Nu = \frac{q_w L}{k_f(T_w - T_\infty)}, \qquad (23)$$

where the heat flux at the surface q_w is define as

$$q_w = -k_{eff}\frac{\partial T}{\partial Y}\bigg|_{Y=0}. \qquad (24)$$

Using similarity variables conveniently we can write

$$Nu = -\frac{K_{eff}}{K_f}\theta'(0). \qquad (25)$$

It must be noted that the effective flow quantities have been taken into account in the evaluation of these quantities. Therefore, it will be more appropriate to name these quantities as the effective skin friction coefficient and the effective Nusselt number. Linear regression is performed on the obtained numerical data to develop the correlation expressions for effective skin friction coefficient and the

effective Nusselt number.

4. Results and Discussion

This section is explicitly prepared to examine the numerical results with the aid of graphs. Plots for velocity, temperature, skin friction coefficient and Nusselt number are presented and analyzed.

Figures 2-4 have been plotted to study the behavior of velocity profile for variation in modified Hartmann number

(Z), variable viscosity parameter (α) and nanoparticles volume fraction (ϕ). Figure 3 depicts that the velocity profile increases with an increase in the modified Hartman number. Such increase is large near the Riga plate and it reduces smoothly as the distance from the plate increases. This observation highlights that the direction and magnitude of applied magnetic field largely alters the velocity of nanofluid. Figure 3 presents the effects of 'α' on velocity profile. This figure shows that velocity of nanofluid increases with an increase in 'α'. Such increase is large
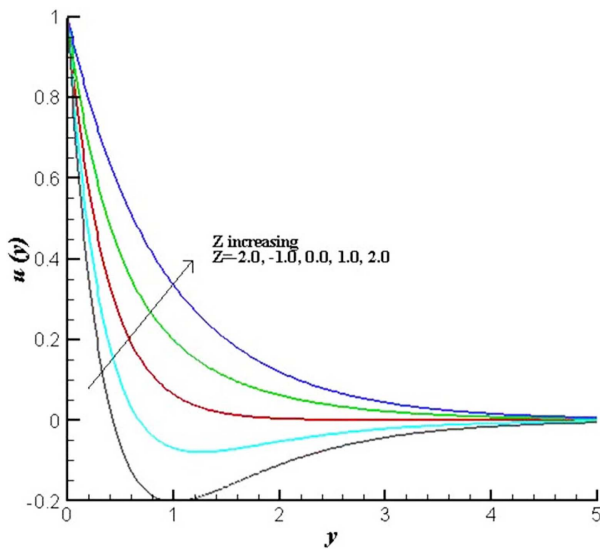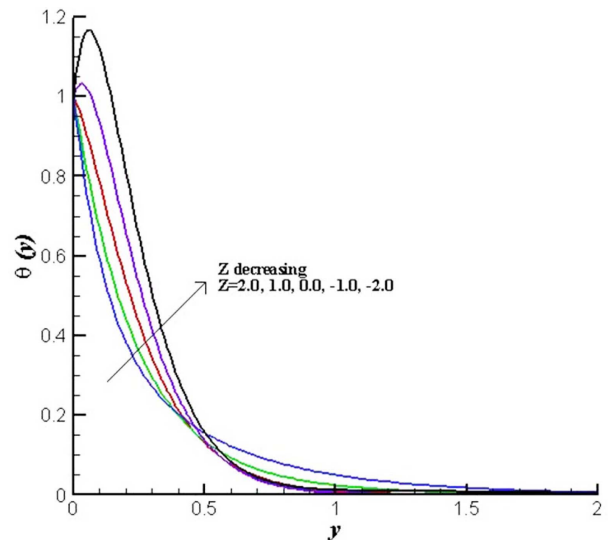

Fig. 2. (Color online) Velocity of water based nanofluid containing copper particles for varying Riga plate parameter Z with $s = 2$, $\lambda = 0.5$, Pr = 6.2, $\phi = 0.1$, $\alpha = 0.1$, $n = 3$.
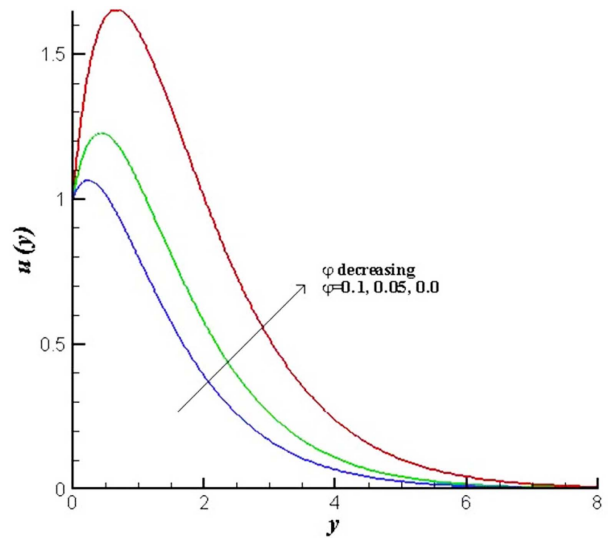
Fig. 4. (Color online) Velocity of water based nanofluid containing copper particles for varying ϕ with $s = 1.0$, $\lambda = 0.5$, Pr = 6.2, $\alpha = 0.3$, $Z = 2.0$, $n = 3$.
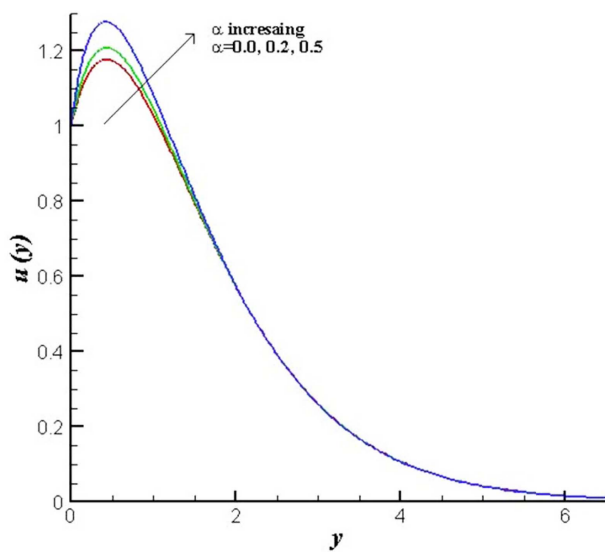
Fig. 3. (Color online) Velocity of water based nanofluid containing copper particles for varying α with $s = 1.0$, $\lambda = 0.5$, Pr = 6.2, $\phi = 0.05$, $Z = 2.0$, $n = 3$.
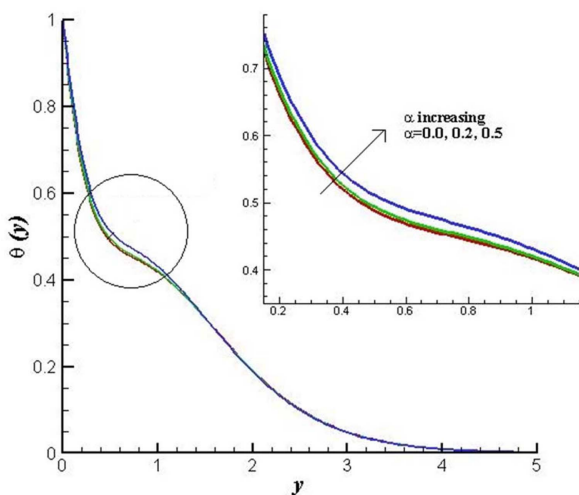

Fig. 5. (Color online) Temperature profile of water based nanofluid containing copper particles for varying Riga plate parameter Z with $s = 2$, $\lambda = 0.5$, Pr = 6.2, $\phi = 0.1$, $\alpha = 0.1$, $n = 3$.
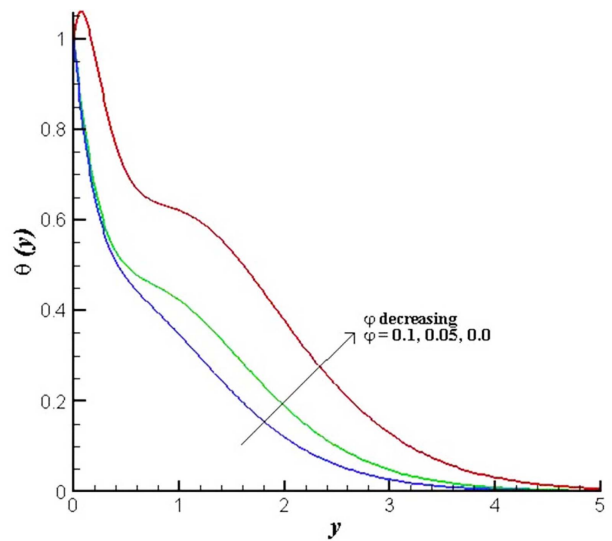
near the Riga plate. Moreover, it is also deduced from this figure that the velocity of nanofluid with constant viscosity is less than that of nanofluid with temperature dependent viscosity. Copper-water nanofluid moves slowly in comparison to pure water (see Fig. 4). Velocity of nanofluid decreases by increasing 'ϕ'. This fact indicates that the addition of copper nanoparticles not only will influence the thermodynamics but also the mechanics of flow. Further it is noted that the boundary layer thickness decreases with an increase in 'ϕ'. Hence copper nanoparticles can be used to control the boundary layer thickness.

Variations in temperature profile are studied through Figs. 5-7. Temperature of nanofluid increases by increasing modified Hartmann number (see Fig. 5). Whereas this observation is reversed as the distance from the plate increases. Hence an increase in the strength of applied magnetic field influences the temperature of nanofluid. Variable viscosity also influences the temperature of nanofluid (see Fig. 6). This Fig. indicates that the temperature of nanofluid increases by a small amount when 'α' is increased. Figure 6 depicts that the temperature of copper-water nanofluid decreases considerably when the nanoparticles volume fraction is increased. This figure also indicates that the ordinary water has higher temperature compared with that of copper-water nanofluid. This fact highlights the use of copper nanoparticles as coolants.
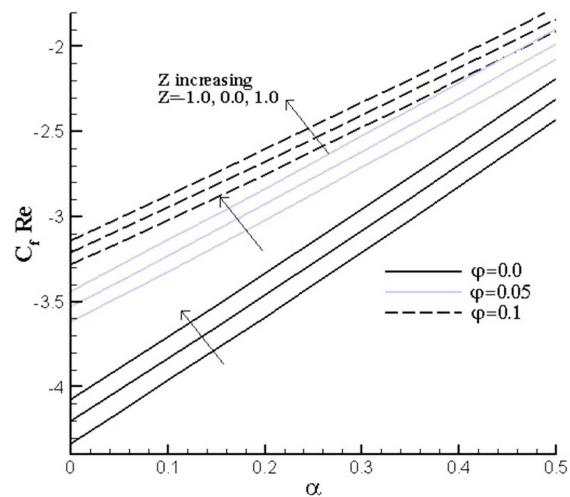
The effective skin friction coefficient and the effective Nusselt number are plotted in Figs. 8 and 9 for variations in embedded parameters. It is observed through Fig. 8

Fig. 7. (Color online) Temperature profile of water based nanofluid containing copper particles for varying ϕ with $s = 1.0$, $\lambda = 0.5$, Pr = 6.2, $\alpha = 0.3$, Z = 2.0, $n = 3$.

Fig. 8. (Color online) Skin friction with $s = 1.0$, $\lambda = 0.5$, Pr = 6.2, $n = 3$.


Fig. 6. (Color online) Temperature profile of water based nanofluid containing copper particles for varying α with $s = 1.0$, $\lambda = 0.5$, Pr = 6.2, $\phi = 0.05$, Z = 2.0, $n = 3$. Encircled part of profile is magnified in small sub-figure for detailed analysis.

that the effective skin friction coefficient increases with an increase in the nanoparticles volume fraction. Also the water free of copper nanoparticles possesses lower values of effective skin friction coefficient when compared with that of copper-water nanofluid. Moreover, an increase in the modified Hartmann number results in an increase in the effective skin friction coefficient. This figure also indicates that the effective skin friction coefficient is small for nanofluid with constant viscosity and it increases with an increase in 'α'. Such increase is uniform and linear. An analytical expression in the form of Riga plate parameter (Z), nanoparticles volume fraction (ϕ) and variable thermal properties parameter (α) to estimate the skin
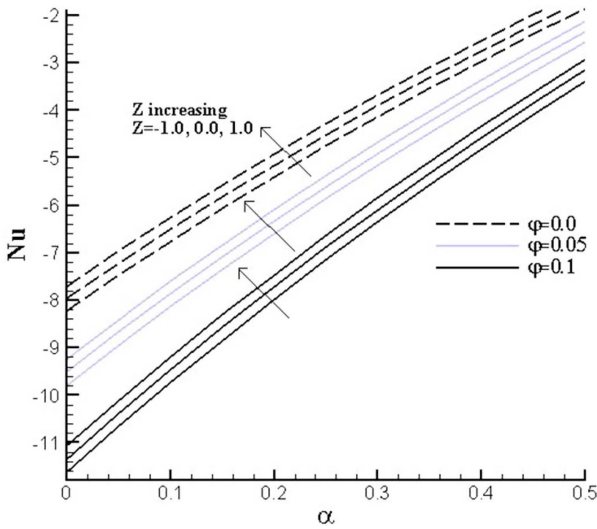
Fig. 9. (Color online) Nusselt number for $s = 1.0$, $\lambda = 0.5$, $Pr = 6.2$, $n = 3$.

friction for copper-water nanofluid with $s = 1.0$, $\lambda = 0.5$ and $n = 3$ is given by:

$$Sf = -4.01 + 2.696\alpha + 8.688\phi + 0.091Z$$

The above expression is obtained performing linear regression on numerical data for 1900 different values for α, ϕ and Z. The maximum percentage error between numerical and estimated values is less than 5 % for α, ϕ in the interval (0.0, 0.1) and Z in the interval (−5.0, 5.0). This correlated expression exhibit that the rate of change of skin friction with respect to ϕ is much prominent when compared with that for other two parameters. Also rate of change in skin friction with respect to α, ϕ and Z is positive, which can also be seen from Fig. 7. In Table 1 correlation of skin friction for different values of λ and s are presented with corresponding maximum percentage error.

Similarly, an expression for effective Nusselt number for the same range of parameters α, ϕ and Z with $s = 1.0$, $\lambda = 0.5$ and $n = 3$ is

Table 1. Correlation of skin friction ($Sf = C + C_a\alpha + C_p\phi + C_zZ$) and maximum percentage error define as [$|Sf_{est} − Sf|/Sf$]100 for different values of λ and suction parameter where the values of α, ϕ is consider in the interval (0.0, 0.1) and Z in the interval (−5.0, 5.0).

λ	s	C	C_a	C_p	C_z	Max. % error
0.0	2.0	−4.694	2.129	8.732	0.096	5.0605
2.0	3.0	−5.061	1.527	7.7	0.1	4.119657
3.0	1.0	−3.667	2.559	7.489	0.091	4.94514

Table 2. Correlation of Nusselt number ($Nu = C + C_{Nb}N_b + C_{Nt}N_t$) and maximum percentage error define as [$|Nu_{est} − Nu|/Nu$]100 for different values of λ and suction parameter where the values of α, ϕ is consider in the interval (0.0, 0.1) and Z in the interval (−5.0, 5.0).

λ	s	C	C_a	C_p	C_z	Max. % error
0.0	2.0	−6.280	11.854	−70.109	0.309	3.372263
2.0	3.0	−2.618	10.213	−86.44	0.333	3.839114
3.0	1.0	−7.306	12.348	−49.839	0.250	4.840463

$$Nu = -7.952 + 12.610\alpha + -51.336\phi + 0.272Z ,$$

with maximum percentage error less than 1. The above expression depicts that the rate of change of Nusselt number with respect to α and Z is positive whereas the rate of change with respect to ϕ is negative. The same behavior of Nusselt number can be observed from Fig. 9. In Table 2 the constants of the correlation expression for Nusselt number different values of λ and s are given.

5. Concluding Remarks

Electro-magnetic mixed convection boundary layer flow of copper-water nanofluid with weakly conducting base fluid induced by a Riga-plate is studied. Key findings of this study are summarized below:

- Velocity of the copper-water nanofluid increases near the Riga plate with an increase in the value of modified Hartmann number.
- Temperature dependent viscosity alters the velocity as well as the temperature of the nanofluid and is of considerable importance in the processes where high accuracy is desired.
- Increase in the effective skin friction coefficient and effective Nusselt number is noted for large values of viscosity parameter.
- Velocity and temperature of the nanofluid decrease with an increase in the nanoparticles volume fraction.
- Addition of copper nanoparticles makes the momentum boundary layer thinner whereas viscosity parameter does not affect the boundary layer thickness.
- It is observed that rate of change in effective skin friction coefficient with respect to α, ϕ and Z is positive and rate of change with respect to nanoparticles fraction is much prominent compared to others.
- Moreover, rate of change in effective Nusselt number with respect to α and Z is positive whereas it is negative with respect to ϕ with prominent magnitude as compare to change with respect to α and Z.

References

[1] S. U. S. Choi, J. Heat Transfer **66**, 99 (1995).

[2] J. Buongiorno, J. Heat Transfer **128**, 240 (2006).

[3] S. Dong, L. Zheng, X. Zhang, and P. Lin, Microfluid Nanofluidics **17**, 253 (2014).

[4] M. Sheikholeslami and D. D. Ganji, J. Mol. Liq. **224**, 526 (2016).

[5] M. Sheikholeslami, Soheil Soleimani, and D. D. Ganji, J. Mol. Liq. **213**, 153 (2016).

[6] M. J. Uddin, O. A. Beg, and A. Ismail, International Journal of Numerical Methods for Heat & Fluid Flow **26**, 5 (2016).

[7] G. K. Ramesh, B. J. Gireesha, and C. S. Bagewadi, Int. J. Heat. Mass. Transf. **55**, 4900 (2015).

[8] J. Sui, L. Zheng, and X. Zhang, Int. J. Therm. Sci. **104**, 461 (2016).

[9] F. M. Abbasi, T. Hayat, and B. Ahmad, Physica E **67**, 47 (2015).

[10] F. M. Abbasi, T. Hayat, and A. Alsaedi, Physica E **68**, 123 (2015).

[11] Mohsen Sheikholeslami, J. Magn. Magn. Mater. **225**, 903 (2017).

[12] Mohsen Sheikholeslami, J. Phys. A, **381**, 494 (2017).

[13] A. Gailitis and O. Lielausis, Appl. Magnetohydrodyn. **12**, 143 (1961).

[14] E. Grinberg, Appl. Magnetohydrodyn. Rep. Phys. Inst. Riga. **12**, 147 (1961).

[15] A. Ahmed, S. Asghar, and S. Afzal, J. Magn. Magn. Mater. **402**, 44 (2016).

[16] H. C. Brinkman, J. Chem. Phys. **20**, 571 (1952).

[17] A. Pantokratoras, Mathematical Problems in Engineering (2008) 149272.